AIP Advances

Analysis of the scintillation mechanism in a pressurized 4He fast neutron detector using pulse shape fitting

R.P. Kelley, D. Murer, H. Ray, and K.A. Jordan

Citation: AIP Advances **5**, 037144 (2015); doi: 10.1063/1.4916904
View online: http://dx.doi.org/10.1063/1.4916904
View Table of Contents: http://scitation.aip.org/content/aip/journal/adva/5/3?ver=pdfcov
Published by the AIP Publishing

AIP ADVANCES **5**, 037144 (2015)

Analysis of the scintillation mechanism in a pressurized ^{4}He fast neutron detector using pulse shape fitting

R.P. Kelley,[1,a] D. Murer,[2] H. Ray,[1] and K.A. Jordan[1]
[1]*University of Florida, Nuclear Engineering Program, Gainesville, FL 32611-6400, USA*
[2]*Arktis Radiation Detectors Ltd., Räffelstrasse 11, 8045 Zürich, Switzerland*

(Received 10 February 2015; accepted 19 March 2015; published online 31 March 2015)

An empirical investigation of the scintillation mechanism in a pressurized ^{4}He gas fast neutron detector was conducted using pulse shape fitting. Scintillation signals from neutron interactions were measured and averaged to produce a single generic neutron pulse shape from both a ^{252}Cf spontaneous fission source and a (d,d) neutron generator. An expression for light output over time was then developed by treating the decay of helium excited states in the same manner as the decay of radioactive isotopes. This pulse shape expression was fitted to the measured neutron pulse shape using a least-squares optimization algorithm, allowing an empirical analysis of the mechanism of scintillation inside the ^{4}He detector. A further understanding of this mechanism in the ^{4}He detector will advance the use of this system as a neutron spectrometer. For ^{252}Cf neutrons, the triplet and singlet time constants were found to be 970 ns and 686 ns, respectively. For neutrons from the (d,d) generator, the time constants were found to be 884 ns and 636 ns. Differences were noted in the magnitude of these parameters compared to previously published data, however the general relationships were noted to be the same and checked with expected trends from theory. Of the excited helium states produced from a ^{252}Cf neutron interaction, 76% were found to be born as triplet states, similar to the result from the neutron generator of 71%. The two sources yielded similar pulse shapes despite having very different neutron energy spectra, validating the robustness of the fits across various neutron energies. [http://dx.doi.org/10.1063/1.4916904]

I. INTRODUCTION

The scintillation properties of ^{4}He gas were studied in a high-pressure (150 bar) fast neutron detector.[1] In an effort to more completely understand the mechanism of high-pressure helium gas scintillation, empirical methods were used in order to gain insight regarding the production of light following a neutron scattering interaction.

Several thousand neutron events were measured and averaged in order to produce a single generic neutron scintillation signal. An analytical equation was derived, using radioactive decay as a model for the decay of light-producing excimer states in the helium gas. By using a least-squares algorithm to fit this analytical equation to the measured neutron scintillation signal, ^{4}He scintillation properties were empirically determined, including the excimer time constants and the ratio between triplet and singlet excimer states produced by a neutron interaction. These results are compared to previous investigations of helium scintillation, and provide a useful framework for future characterization efforts.

[a]rpkelley@ufl.edu

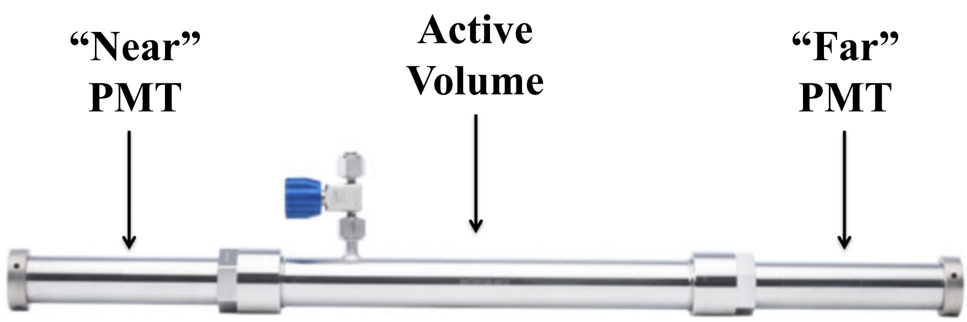

FIG. 1. A ^{4}He detector manufactured by Arktis Radiation Detectors. The active volume is pressurized to 150 bar.

II. ^{4}He DETECTORS

A. Interaction mechanism

The ^{4}He detectors used in these experiments are manufactured by Arktis Radiation Detectors. They are simple in design, as illustrated in Fig. 1, and are manufactured in several sizes. The model used in these measurements had an active length of 20 cm, with an inner diameter of 4.4 cm, giving a total active volume of 304 cm^3. The active volume is filled with pure helium-4 gas, doped with other gases on the ppm scale and pressurized to 150 bar. Photomultiplier tubes (PMTs) operating at 1680 V are mounted at either end of the active volume and measure the scintillation light produced from radiation interactions with the fill gas. The detector body is made of stainless steel.

The operation of the detector is based on the elastic scattering of a fast neutron with the helium fill gas. ^{4}He has a peak in its cross section for elastic scattering around 1 MeV that makes it an excellent medium for the detection of fast neutrons.

The incident neutron transfers a fraction of its kinetic energy to the helium atom, as a function of its scattering angle. This helium atom is stripped of electrons and moves through the gas as a recoil alpha particle. This alpha excites and ionizes other helium atoms along its path of travel through the active volume. The result of these excitations and ionizations is the production of singlet and triplet excited states (excimers). As these excimers decay to the ground state, they give off scintillation light, which is measured by the PMTs at each end of the detector. An example of a single event output trace is shown in Fig. 2.

Fig. 2 shows that the trace can be separated in time into two components. The fast component is a sharp peak that exists on the order of nanoseconds; the slow component is a series of smaller pulses, stretched out over four microseconds. This work will investigate if the time separation in the scintillation signal is due to differences in the decay mechanisms of the singlet and triplet excimer states, and therefore it is useful to explore this process in more detail.

B. Helium scintillation

In its ground state, ^{4}He has two electrons that occupy its 1s orbital and have opposite spin states. In the singlet excimer state, one of these electrons is promoted to a higher orbital, and therefore a higher energy level, but still retains its original spin orientation. In a triplet excimer state, however, the excited electron is not only promoted to a higher energy orbital, but also reverses its spin state. Therefore the end result is a helium atom with electrons in two different orbitals, but with the same spin state.[2] The work of Dennis et al. noted that triplet states are three times more likely to be produced than singlet states.[3]

The processes of decay for these excimers result in important scintillation signal effects. A singlet excimer state will undergo radiative decay by emission of a photon (scintillation). This photon will have an energy of 16 eV (wavelength ~80 nm).[4] The decay of a triplet state, on the other hand, requires the excited electron to reverse its spin state, thereby becoming a singlet state. This singlet state then decays by the same photon emission process described above. The end result of

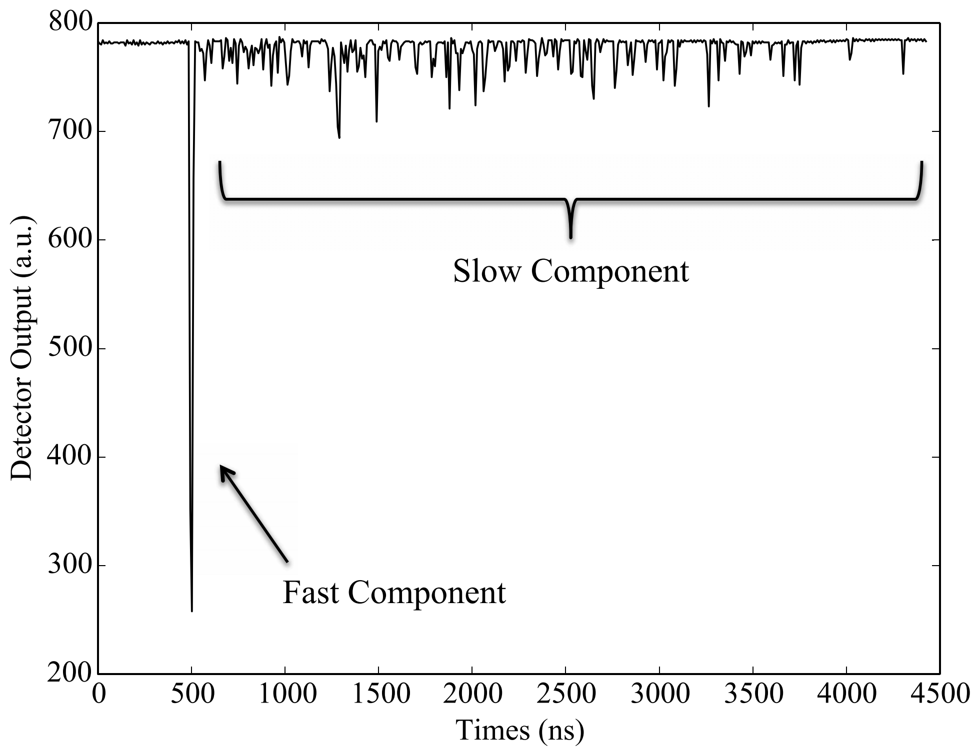

FIG. 2. ^{4}He detector output for a single neutron event, highlighting the slow and fast components.

these various scintillation processes is the emission of approximately 15,000 photons per MeV of deposited energy.[1]

Since the triplet decay mode depends on the reversal of an electron spin, its probability of occurrence is reduced, resulting in a longer-lived triplet excimer state compared to singlet states. Due to these time differences in their rates of decay, the singlet excimer states are responsible for the formation of the fast scintillation component, and the triplet excimer states are responsible for the formation of the slow scintillation component. Together, these two components make up the resulting raw signal trace.

III. EXPERIMENTAL METHODS

Two different neutron sources were used in these experiments: a ^{252}Cf spontaneous fission source, which produces neutrons over an energy spectrum up to 10 MeV, and a deuterium-deuterium (d,d) neutron generator, which induces the fusion of deuterium atoms to produce mono-energetic neutrons at 2.45 MeV.

The ^{252}Cf measurements were conducted using a single ^{4}He detector, and a 200 μCi ^{252}Cf spontaneous fission source at a distance of 40 cm from the center of the detector's active volume. In order to reduce the number of incident gamma rays, a 5 cm-thick lead shield was placed between the source and the detector, reducing the observed detector count rate from 259 to 105 events per second. Five thousand detector events were recorded in this manner, a quantity that was shown to give acceptable uncertainties in the final results.

The neutron generator measurements were also conducted using a single ^{4}He detector, at a distance of 380 cm from the generator. Lead shielding was not used in this measurement, since the neutron generator produces x-rays which are shielded by the stainless steel in both the generator pressure vessel and the detector housing. Five thousand events were also recorded in this configuration.

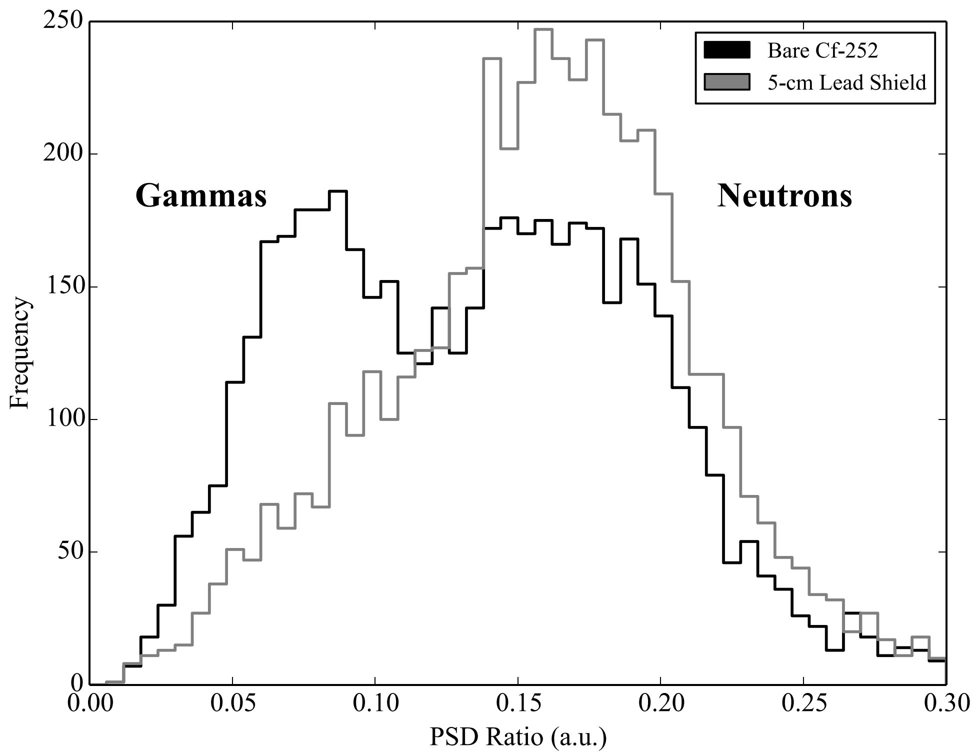

FIG. 3. The distribution of the ratio between the slow and fast components, shown for both a bare and shielded ^{252}Cf measurement.

Pulse shape discrimination (PSD) was then applied to further reduce the number of gamma events. Previous work has shown that the intensity of the light in the slow component of a neutron event is up to eight times greater than the light in the slow component of a gamma event.[1] For each event, the ratio between the intensity of the slow and fast component is computed, and shows good separation between neutron and gamma events. Figure 3 shows the distribution of this PSD ratio for both a bare ^{252}Cf measurement and a measurement with a 5 cm lead shield. The bare ^{252}Cf distribution illustrates that this technique provides effective separation between neutrons and gammas, while the distribution from the lead shield shows the effectiveness of the 5 cm lead shield in reducing the fraction of gamma events.

After plotting each event by its slow and fast component, a straight-line PSD algorithm was used to separate neutrons and gammas, as illustrated by the thick line in Fig. 4. Events above this PSD calibration line were retained as neutrons, while events below the line were discarded as gammas. To quantify the gamma rejection capabilities of this method, Fig. 4 shows two separate measurements using a ^{252}Cf neutron/gamma source (white) and a ^{60}Co gamma source (gray). The black markers represent gamma events with an integrated slow component that was sufficiently high for that event to fall above the line and therefore be misclassified by the PSD algorithm as a neutron event. This calibration measurement showed that 1.5% of the ^{60}Co gamma events were erroneously classified as neutrons.

The actual application of this PSD process to the ^{252}Cf data gathered for this experiment is shown in Fig. 5. Events retained as neutrons are shown in white, while events discarded as gammas are shown in black. Of the original 5,000 detector events recorded in this configuration, 2,830 were retained as neutrons (57%). Applying the same method to the neutron generator measurements, only 1,905 events were retained as neutrons (38%). The higher fraction of gammas in this configuration is due to the absence of the lead shielding used in the ^{252}Cf measurements.

Figure 5 shows that at lower slow/fast component intensities, there is significantly less distinction between neutron and gamma events. In order to further ensure the removal of gamma events

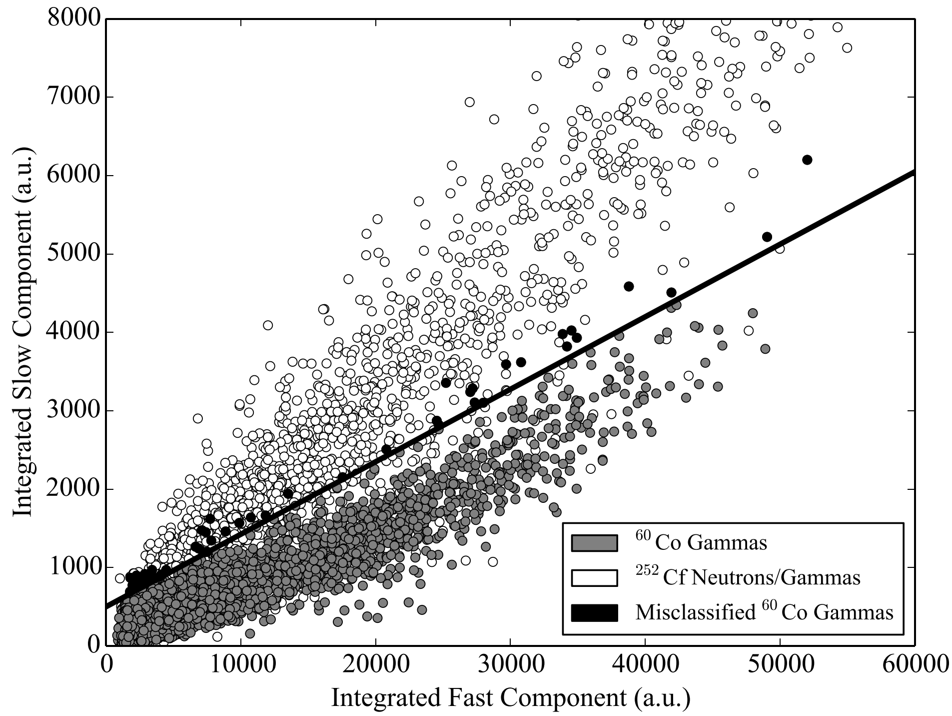

FIG. 4. A ^{252}Cf neutron/gamma measurement (white) overlaid with a ^{60}Co gamma measurement (gray), which was used to select the points of the PSD line and to quantify the fraction of misclassified gammas (1.5%).

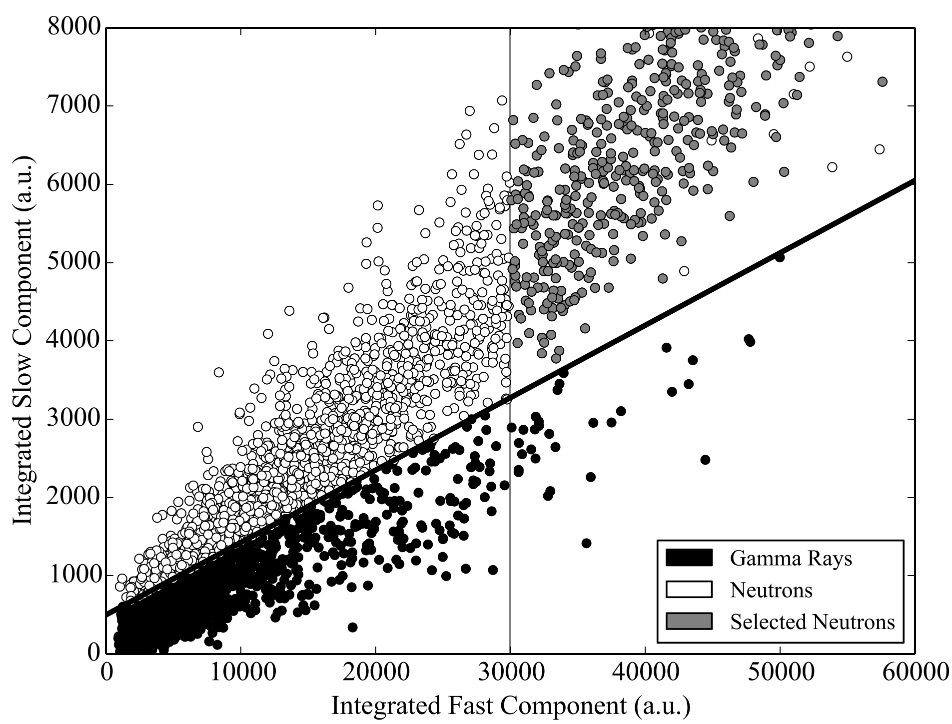

FIG. 5. An illustration of the selection process. The thick calibration line was used for pulse shape discrimination between neutron (white) and gamma events (black), while the thin vertical line represents a fast component cutoff. Gray circles indicate neutrons retained for averaging.

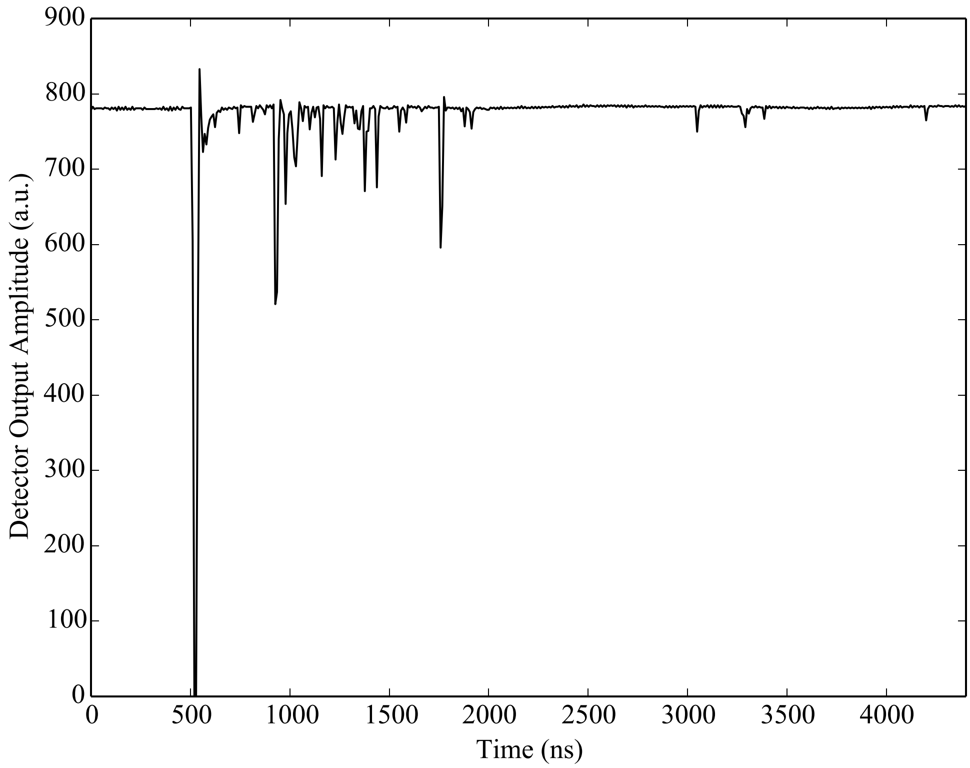

FIG. 6. A detector output trace where the fast component is saturated. This type of truncated event was discarded from the sample set.

from the sample set, a fast component cutoff was implemented at 30,000 (intensity of the fast component in arbitrary detector output units), illustrated by the thin vertical line in Fig. 5. This cutoff was chosen based on the results of the calibration measurement discussed in Fig. 4, which showed this method reduced the fraction of misclassified gammas to 0.3%.

The final step in the selection process was ensuring that events above this cutoff were not saturated. As shown in Fig. 6, higher-energy events can saturate the maximum pulse height which is recorded by the PMTs, thereby truncating the peak of the pulse and artificially altering the pulse shape. Since the raw pulse shape must be preserved for the subsequent analyses, saturated events were identified and discarded.

Of the 2,830 ^{252}Cf events that were retained as neutrons, 597 were retained as being both above the fast component cutoff and non-saturated (21%), and was therefore the final size of the sample set used for the subsequent analyses (12% of the original 5,000 events). These retained events are shown in gray in Fig. 5. For the neutron generator measurement, 424 of the 1,905 events retained by the PSD algorithm were selected for final analysis (9% of the original 5000 events).

IV. ANALYTICAL METHODS

A. Average pulse shape

These selected events were averaged into a single, generic scintillation pulse for each neutron source. A 7-window (61 ns wide) moving average was used to remove statistical variances and further smooth the pulse shapes. Finally, the pulses were inverted and the baseline normalized to zero, for the convenience of subsequent interpretations. The end results are shown in Fig. 7. Despite being from different sources with very different energy spectra, the averaged pulses are similar in shape, validating that the results of subsequent fits are representative across various neutron energies.

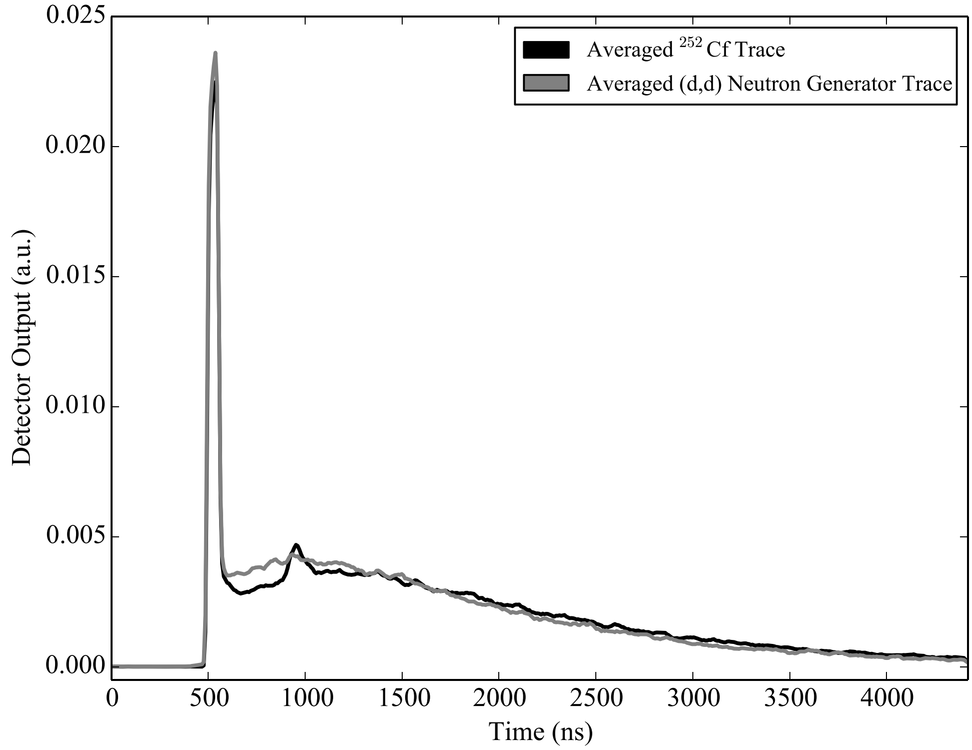

FIG. 7. The average neutron pulse shapes measured from the shielded ^{252}Cf source (black) and the (d,d) neutron generator (gray). The pulses are similar in shape, validating the robustness of the analysis method across different sources.

B. Mathematical model of scintillation

In order to analyze the scintillation mechanism in the ^{4}He fill gas, a mathematical model of scintillation was derived. This equation describes the production of light in the detector as a function of time after a neutron interaction. Fitting this model to the average measured scintillation signal allows for an empirical analysis of the scintillation mechanism and the helium excimer states. The equation was derived in the following manner by modeling the decay of the helium excimer states on the decay of radioactive isotopes.

As described above, an interaction in the ^{4}He fill gas produces both singlet and triplet excimer states. The initial populations for each of these states are denoted as N_S^o and N_T^o, respectively. These initial populations are assumed to be produced instantaneously.

The rate of change of the population of the singlet excimer states can be written as:

$$\frac{dN_S}{dt} = \lambda_T N_T - \lambda_S N_S, \tag{1}$$

Where the first term represents the production of singlet states due to the decay of triplet states, and the second term represents the decay of singlets to the ground state, which results in the production of scintillation light. The triplet and singlet decay constants are given by λ_T and λ_S, respectively.

The triplet population at time t ($N_T(t)$) can be written as:

$$N_T(t) = N_T^o e^{-\lambda_T t}. \tag{2}$$

Substituting Eq. (2) into Eq. (1) and re-arranging gives:

$$\frac{dN_S}{dt} + \lambda_S N_S - \lambda_T N_T^o e^{-\lambda_T t} = 0. \tag{3}$$

Eq. (3) is a first-order differential equation with the solution:

$$N_S(t) = \frac{\lambda_T}{\lambda_S - \lambda_T} N_T^o (e^{-\lambda_T t} - e^{-\lambda_S t}) + N_S^o e^{-\lambda_S t}, \tag{4}$$

In which the second term is the contribution from singlet states produced directly from the interaction at $t = 0$.

The rate of decay of singlet states to produce light can be represented by the treating the singlet states as radioactive isotopes and calculating their activity:

$$L = A_S = \lambda_S N_S, \tag{5}$$

$$L(t) = \frac{\lambda_S \lambda_T}{\lambda_S - \lambda_T} N_T^o (e^{-\lambda_T t} - e^{-\lambda_S t}) + \lambda_S N_S^o e^{-\lambda_S t}. \tag{6}$$

It is also useful to define the total light output. Since all excimers that were produced from the interaction must ultimately decay, we can represent this total light output ζ by the sum of the excimer states initially produced:

$$\zeta = N_T^o + N_S^o, \tag{7}$$

And the fraction of excimer states that are produced from an interaction as long-lived triplet states F by:

$$F = \frac{N_T^o}{N_T^o + N_S^o}. \tag{8}$$

We can now re-write N_T^o and N_S^o in terms of F and ζ:

$$N_T^o = F\zeta, \tag{9}$$

$$N_S^o = (1 - F)\zeta. \tag{10}$$

Substituting these relationships into Eq. (6) gives:

$$L(t) = \frac{\lambda_S \lambda_T}{\lambda_S - \lambda_T} F\zeta (e^{-\lambda_T t} - e^{-\lambda_S t}) + \lambda_S (1 - F)\zeta\, e^{-\lambda_S t}, \tag{11}$$

Which, after grouping the exponential terms together, becomes:

$$L(t) = \frac{\lambda_S F\zeta}{\lambda_S - \lambda_T} \lambda_T e^{-\lambda_T t} + \zeta \left[(1 - F) - \frac{F\lambda_T}{\lambda_S - \lambda_T} \right] \lambda_S e^{-\lambda_S t}. \tag{12}$$

This equation models the production of scintillation light, but is an ideal model in that it fails to account for the differences in processing time that result from the detector electronics. The total time taken for the detector to measure the scintillation response from a particle interaction is the sum of multiple signal processing steps. These steps include the time it takes for the recoil alpha particle to travel through the gas after a scattering interaction, the movement of scintillation light along the detector volume to the PMT photocathodes, as well as the movement of electrons through the various dynode stages in the PMT.[5] Each of these individual steps will have its own amount of random deviation, and this deviation will cause a distortion of the measured scintillation signal. The overall distribution of the variation of these individual steps can be represented using a Gaussian resolution function, defined by a mean transmission time μ and a standard deviation σ.

The convolution of this Gaussian resolution function with the exponential scintillation equation (Eq. (12)) produces what is known as the ex-Gaussian (exponentially-modified Gaussian) distribution.[6] The ex-Gaussian is given by:

$$f(t, \lambda) = \frac{1}{\tau} e^{\left[\frac{\mu - t}{\tau} + \frac{\sigma^2}{2\tau^2}\right]} \cdot \Phi \left[\frac{t - \mu}{\sigma} - \frac{\sigma}{\tau} \right], \tag{13}$$

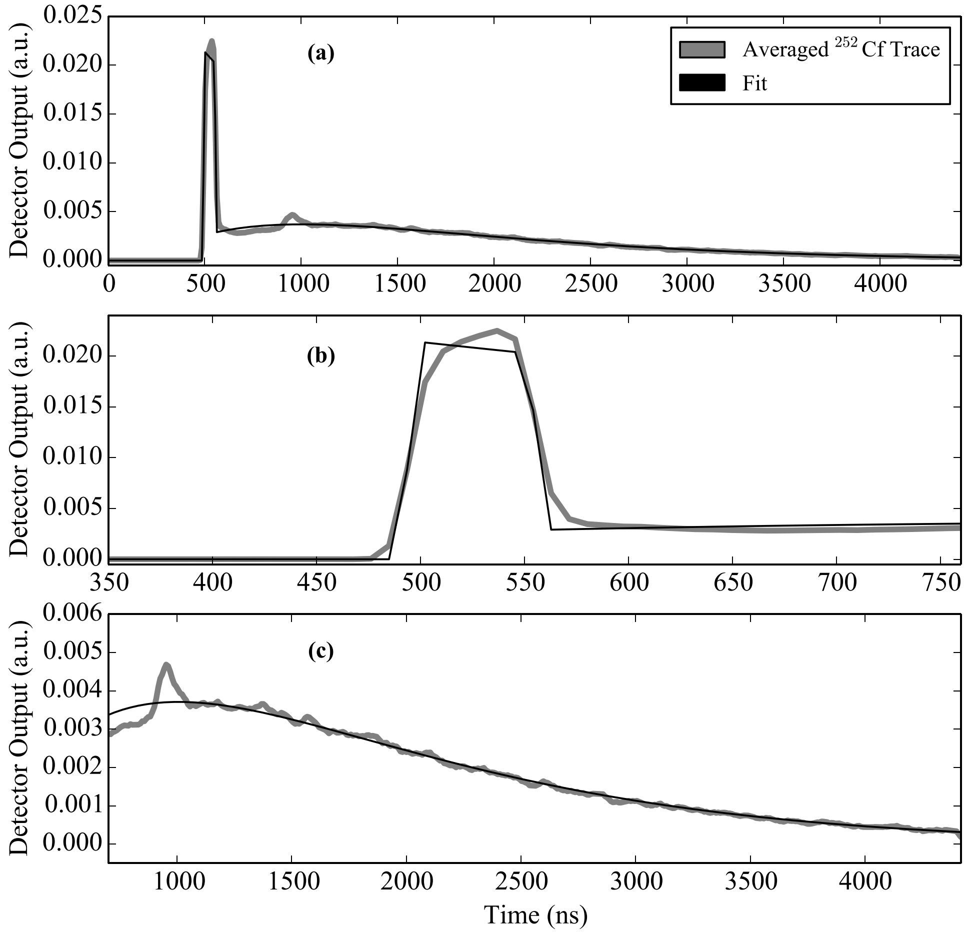

FIG. 8. (a) For the ^{252}Cf source, the result of fitting the derived pulse shape function (black) to the measured neutron pulse (gray). Also shown are magnified views of the fast (b) and slow (c) component time scales.

Where Φ is the normal cumulative distribution function (CDF) and τ is the excimer time constant, which is the inverse of the decay constant λ. Substituting the ex-Gaussian yields the final expression for the pulse shape over time:

$$L(t) = \frac{\lambda_S F \zeta}{\lambda_S - \lambda_T} f(t, \lambda_T) + \zeta \left[(1 - F) - \frac{F \lambda_T}{\lambda_S - \lambda_T} \right] f(t, \lambda_S). \tag{14}$$

V. RESULTS & DISCUSSION

The scintillation model (Eq. (14)) was fitted to each of the average neutron pulses presented in Section IV A using a least-squares optimization algorithm. The algorithm used the Levenburg-Marquardt gradient method to minimize the sum of the squared errors between the provided average neutron pulse shape and the pulse shape resulting from the fit parameters.[7,8] It is critical to note that these types of algorithms lack robustness, in that the gradient method will always trend towards the nearest local minimum, which is not necessarily the global minimum. The selection of initial guess parameters therefore becomes important, since they determine where the algorithm will begin its search and therefore its proximity to the true global minimum. The initial parameters were selected for this study by trial and error runs, in which the parameters were manually adjusted

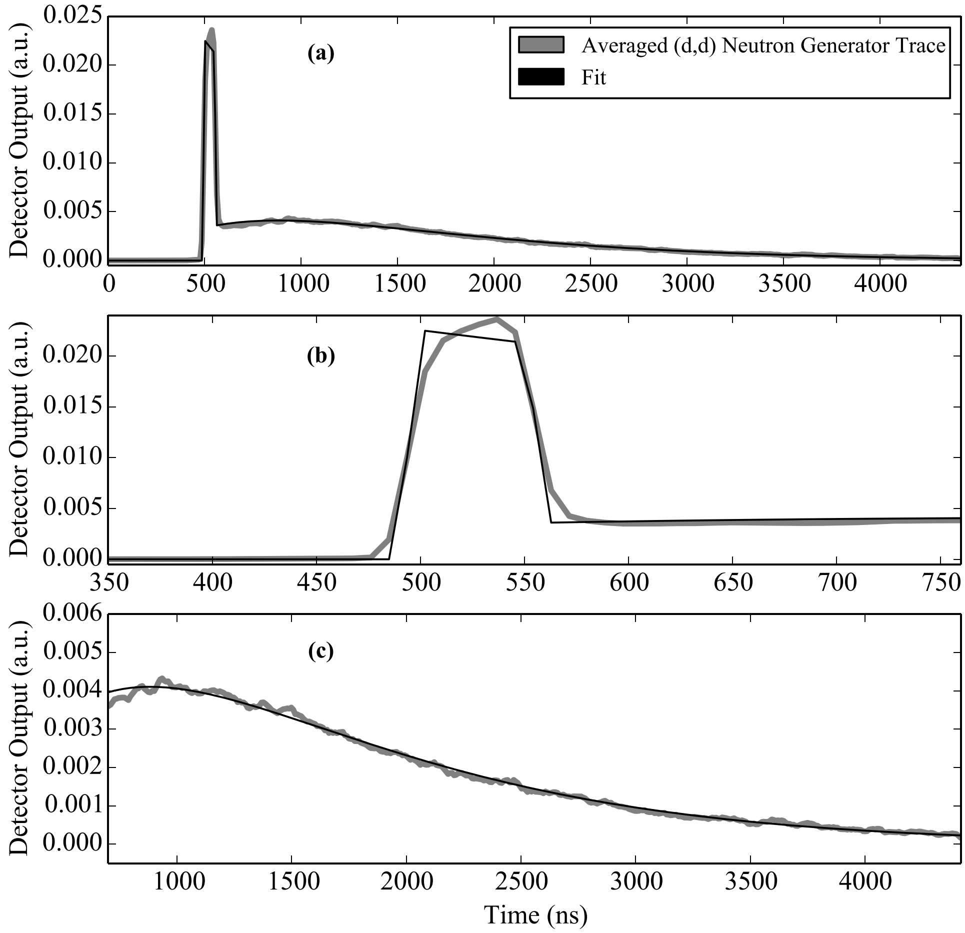

FIG. 9. (a) For the (d,d) neutron generator, the result of fitting the derived pulse shape function (black) to the measured neutron pulse (gray). Also shown are magnified views of the fast (b) and slow (c) component time scales.

until the least-squares algorithm was able to achieve a reasonable fit to the measured pulse shape. Despite being subjective, the method proved sufficient for identifying a good starting point for the algorithm.

The result of the ^{252}Cf fit is shown in Fig. 8, where the measured neutron pulse shape is shown in gray and the fitted pulse shape is shown in black. Similarly, the neutron generator fit result is shown in Fig. 9. Each fit can be seen to reproduce the measured neutron shape well.

The results from fitting the scintillation time constants to the measured pulse shapes are summarized in Table I, including the corresponding decay constants and scintillation half-lives. It was described in Section II B that the excimer transition from the triplet state to the singlet state takes longer than the transition from singlet state to ground, due to quantum mechanical effects. The empirical results of the ^{252}Cf pulse shape fitting support this: the triplet time constant τ_T and the singlet time constant τ_S were 970 ns and 686 ns, respectively. Similar time constants were found with the neutron generator pulse shape fitting: 884 ns (τ_T) and 636 ns (τ_S). The results of the pulse shape fitting confirm that the triplet states have a longer life than singlet states.

Although these results match the expected response in that it shows the triplet excimer states decay slower than the singlet excimer states, the magnitude of the difference varies significantly from previous research on the mechanism of helium scintillation. Hill, for example, concluded that the decay time for a helium singlet state was 0.55 ns.[9] Kopeliovich et al.[10] and Chabalowski et al.[11] both conducted investigations on the decay of the triplet states and obtained decay times of 15 s and 18 s, respectively. The trend in these previous works maintains the expectation expressed earlier,

TABLE I. Values of the scintillation parameters determined by the pulse shape fitting.

			^{252}Cf		(d,d)	
Parameter	Symbol	Units	Singlet	Triplet	Singlet	Triplet
Time Constant	τ	ns	686	970	636	884
Decay Constant	λ	μs^{-1}	1.46	1.03	1.57	1.13
Half-Life	$t_{1/2}$	ns	475	672	441	613

that the triplet states decay slower than the singlet states, but differ by two orders of magnitude from the results of this pulse shape study.

The differences between the results presented here and previous helium scintillation research arise from differences in the experimental configurations. For example, previous research does not use high-purity ^{4}He as the fill gas. More importantly, previous research was conducted across much lower pressure ranges. The work of Kopeliovich et al., for example, was conducted over the pressure range of 25 to 40 atm,[10] while the Arktis ^{4}He detectors used in this research were pressurized to 150 atm. Since the work of Konovalov[12] and Kubota[13] have both demonstrated that the scintillation response, including the excimer decay times, is dependent upon the gas pressure, this is most likely the primary explanation for the variations in the results.

Another important outcome of the ^{252}Cf pulse shape fitting analysis was that 76% of the excimers produced from a neutron interaction were born as triplet states. A smaller fraction (24%) of excited states are therefore born as singlet states. Similarly, the neutron generator fit showed that 71% of the excimers were born as triplets (29% born as singlets). These results check with the expectation described in Section II B that the initial excimer population resulting from the excitations and ionizations of the high-pressure helium fill gas consists mostly of triplet states. Moreover, these results match the work of Dennis et al., which noted that triplet and singlet excimer states are populated according to a 3:1 statistical weight.[3] Dennis et al. also observed that as the density of the scintillator was increased, there was a distinct shift toward the population of a higher fraction of singlet states. Comparing the results of this helium gas study to a previous study using pulse shape fitting to examine the scintillation mechanism in plastic scintillators supports this observation, in that the denser plastic scintillator was found to have an initial triplet fraction of 25.5% in that work.[14]

For the ^{252}Cf fit, the mean transmission time μ and the standard deviation σ of the Gaussian resolution function were calculated to be 347 ns and 378 ns, respectively (338 ns and 371 ns for the neutron generator fit). For this study the mean transmission time is a measure of the delay between the production of scintillation light in the detector and the arrival of the signal at the measurement device. Therefore the final value of the delay parameter is arbitrary in that it does not affect the actual shape of the signal, only the position of the start of the scintillation pulse along the x-axis. The standard deviation of the resolution function, on the other hand, is a measure of the spread of the transmission times of the signal through the various processing stages discussed in Section IV B, and therefore has a direct effect on the overall shape of the scintillation signal.

VI. CONCLUSIONS

A ^{4}He detector was used to measure neutron events from a ^{252}Cf spontaneous fission source and a (d,d) neutron generator. These events were then averaged and smoothed, producing a single scintillation pulse shape for each source. A mathematical model for the decay of excited helium states and the production of light after a neutron interaction was developed and fitted to the measured neutron pulse shapes using a least-squares optimization algorithm. The algorithm obtained the best fit solution to each pulse by varying physical parameters related to the mechanism of helium scintillation in the detector fill gas, allowing for an empirical analysis.

The results were compared to previous research regarding the scintillation process in helium. Differences were noted in the magnitude of various parameters, including the triplet and singlet time constants, however the general relationships were noted to be the same and checked with expected trends from theory.

ACKNOWLEDGMENTS

This work was funded by a Nuclear Regulatory Commission Graduate Fellowship.

[1] R. Chandra, G. Davatz, H. Friederich, U. Gendotti, and D. Murer, "Fast neutron detection with pressurized 4he scintillation detectors," Journal of Instrumentation **7**, C03035 (2012).
[2] T. Fujisawa, D. G. Austing, Y. Tokura, Y. Hirayama, and S. Tarucha, "Allowed and forbidden transitions in artificial hydrogen and helium atoms," Nature **419**, 278–281 (2002).
[3] W. Dennis, E. Durbin Jr, W. Fitzsimmons, O. Heybey, and G. Walters, "Spectroscopic identification of excited atomic and molecular states in electron-bombarded liquid helium," Physical Review Letters **23**, 1083 (1969).
[4] D. McKinsey, C. Brome, S. Dzhosyuk, R. Golub, K. Habicht, P. Huffman, E. Korobkina, S. Lamoreaux, C. Mattoni, and A. Thompson *et al.*, "Time dependence of liquid-helium fluorescence," Physical Review A **67**, 062716 (2003).
[5] Z. Cao and L. Miller, "Evaluation of pulse shape discrimination performance of scintillation materials and psd methods by using statistical models," Nuclear Instruments and Methods in Physics Research Section A: Accelerators, Spectrometers, Detectors and Associated Equipment **416**, 32–44 (1998).
[6] M. R. Dawson, "Fitting the ex-gaussian equation to reaction time distributions," Behavior Research Methods, Instruments, & Computers **20**, 54–57 (1988).
[7] K. Levenberg, "A method for the solution of certain problems in least squares," Quarterly of applied mathematics **2**, 164–168 (1944).
[8] D. W. Marquardt, "An algorithm for least-squares estimation of nonlinear parameters," Journal of the Society for Industrial & Applied Mathematics **11**, 431–441 (1963).
[9] P. C. Hill, "Ultraviolet continua of helium molecules," Physical Review A **40**, 5006 (1989).
[10] D. Kopeliovich, A. Y. Parshin, and S. Pereverzev, "Spectral properties and the dynamics of of excimer of he? 2 molecules in 4he crystals," Sov. Phys. JETP **69**, 638 (1989).
[11] C. F. Chabalowski, J. O. Jensen, D. R. Yarkony, and B. H. Lengsfield III, "Theoretical study of the radiative lifetime for the spin-forbidden transition a 3σ + u? x 1σ + g in he2," The Journal of Chemical Physics **90**, 2504–2512 (1989).
[12] A. Konovalov and G. Shlyapnikov, "Decay kinetics of triplet he (23s) excitations in liquid and solid helium," Soviet Physics JETP **73**, 286–291 (1991).
[13] S. Kubota, T. Takahashi, and T. Doke, "Mechanism of scintillation of helium, helium-argon, and helium-neon gas mixtures excited by alpha particles," Physical Review **165**, 225 (1968).
[14] N. Hawkes and G. Taylor, "Analysis of the pulse shape mechanism in a plastic scintillator with efficient neutron/gamma pulse shape discrimination," Nuclear Instruments and Methods in Physics Research Section A: Accelerators, Spectrometers, Detectors and Associated Equipment **729**, 522–526 (2013).